

Green Polymer Electrolyte Host Based on Newly Synthesized Benzoyl κ -Carrageenan: Less Hydrophilic and Improved Conductivity

Norsyabila Shrgawi¹ Intan Juliana Shamsudin^{2*} Hussein Hanibah³

Norherdawati Kasim² Siti Aminah Mohd Noor² and Safura Taufik²

¹Faculty of Defence Science and Technology, National Defence University of Malaysia, Sungai Besi Camp, 57000 Kuala Lumpur.

²Centre for Defence Foundation Studies, National Defence University of Malaysia, Sungai Besi Camp, 57000 Kuala Lumpur.

³Centre of Foundation Studies, Universiti Teknologi MARA, Dengkil Campus, 43800 Dengkil Selangor.

*Correspondence: intanjuliana@upnm.edu.my

Abstract: Newly synthesized benzoyl kappa carrageenan (Bz- κ car) has been successfully produced by Friedel Craft acylation method. The successful substitution of benzoyl molecule into kappa carrageenan (κ car) polymeric chain was confirmed by FTIR analysis based on the formation of new carbonyl (C=O) and C=C bonds in Bz- κ car. ¹H-NMR analysis has further proven the benzoylation by the appearance of new multiple resonances peaks at δ =6.6-9.50 ppm belongs to the characteristic signals of protons in aromatic benzoate group. XRD analysis showed reduced crystallinity of the synthesized carrageenan while elemental analyser analysis revealed the increase percentages of carbon in Bz- κ car upon the substitution. Highest degree of substitution obtained is 0.27. TGA showed lower degradation temperature in the synthesized carrageenan while water contact angle analysis demonstrated that Bz- κ car is less hydrophilic compared to the pristine κ car. Solubility tests showed that Bz- κ car is best dissolved in ethylene glycol. The benzoylation has also improved ionic conductivity of Bz- κ car to $3.10 \times 10^{-4} \text{ Scm}^{-1}$ at ambient temperature.

Keywords: carrageenan, electrolyte, benzoyl, hydrophilic, conductivity, acylation.

1.0 Introduction

Kappa-carrageenan (κ car) is an anionic sulfated linear polysaccharide extracted from red seaweed with a linear backbone built of an alternating (1 \rightarrow 3)-linked β -D-galactopyranose and (1 \rightarrow 4)-linked α -D-galactopyranose [1]. *Euचेuma cottonii* is known as the important species that yields κ car [2]. Major applications of κ car include its uses as an additive in the foods industry [3], cosmetic and personal care products [4], and pharmaceutical industry [5]. Special characteristics of κ car involve biocompatibility, biodegradability, high capacity of water retention and mechanical strength of its gel. Over the past decade, the usage of κ car in electrochemistry field has been actively developed and progressing [6, 7]. Recent utilizations of κ car as propitious electrolytes in electrochemical devices were also reported [8].

However, similar to other polysaccharide, the main concern is the high polarity and hydrophilicity of κ car due to the large numbers of hydroxyl group (OH) in its chemical structure [9]. In this case, κ car has strong interactions with water molecules, as the hydroxyl groups are capable to form hydrogen bonds with polar water molecules. Unfortunately, the presence of water/moisture in most of electrochemical devices such as battery and dye-sensitized solar cell is not favorable. The interaction of moisture with air/moisture sensitive metal/parts in the devices might have caused explosion and risking the surrounding. Additionally, the exposure to moisture will lead to corrosion issue in the devices, thus deteriorates and affecting the devices' performance. Chemical modifications on κ car to alter the hydrophilic properties of κ car were previously reported. Recently, in food industry application, hydrophobic modification of κ car microgel particles was performed for the stabilisation of foams [10]. Previously, Tye and co-workers (2018)

performed alkali modification on κ car [11]. The results showed that the alkali-modified κ car exhibited better thermal stability, water vapour barrier property and less hydrophilic as compared to the unmodified carrageenan film. Besides that, study on the synthesis of acylated κ car was reported. Long alkyl chain, decanoyl chloride was used as acylating agent in the synthesis [12]. The hygroscopic nature of the acylated carrageenan was reduced compared to pure carrageenan. However, although all the investigations reported reduced hydrophilicity, no study on the potential of the modified κ car as electrolyte were reported.

Another concern on κ car as polymer host in electrolyte system is its thin film conductivity (σ) is rather low, (10^{-7} S cm^{-1}). Increment in σ is important to be applicable as electrolyte in electrochemical devices. Therefore, studies of synthesized κ car in order to enhance the σ were previously reported. In recent past, succinyl κ car was synthesized by mixing κ car with succinic anhydride $(\text{CH}_2\text{CO})_2\text{O}$ via one-step modification reaction [13]. The substitution of the succinic group into κ car backbone has improved the σ and its interaction with ions compared to its pristine form. In other study, O-methylene phosphonic κ -carrageenan (OMPC) was chemically synthesized via phosphorylation reaction [14]. Methylene phosphonic acid was introduced into carrageenan as a phosphoryl functional group to produce phosphorylated carrageenan. The σ of OMPC film were 1.54×10^{-5} S cm^{-1} , one order of magnitude higher than the pure carrageenan. The authors concluded that the improvement in the σ is due to the oxygen-rich ionogenic group $(-\text{CH}_2\text{PO}_3\text{H}_2)$ substituted into the side chain of κ car. Synthesis of carboxymethyl carrageenan was formerly reported [15]. The substitution of polar group (CH_3COOH) , brought more oxygens in the polymeric matrix, thus provided vacancy for cations to coordinate with the polymer. As a result, the σ was reported to enhance by three orders of magnitude to 2.0×10^{-4} S cm^{-1} , compared to the pure κ car film. Nonetheless, although all the synthesis had successfully increased the σ , with the increase number in the polar groups, the hydrophilic properties were also increased, thus affecting the electrolytes' performance in electrochemical devices.

Therefore, our aim is to modify hydrophilic and low σ κ car into less hydrophilic and conductive benzoyl κ car (Bz- κ car). Here, κ car is synthesized to undergo acylation reaction and benzoyl chloride (BC) acts as the acylating agent. To the best of our knowledge, the investigation on the synthesis of Bz- κ car and its application as polymer host in an electrolyte system has never been reported elsewhere. Thus, this study is expected to give new idea to improve the properties of κ car-based electrolyte specifically, and polysaccharide based electrolyte generally.

2. Materials and methods

2.1 Materials

κ -carrageenan (κ car) powder (molecular weight: 788.7 g/mol) and benzoyl chloride (BC) (purity: 99%) liquid were purchased from Sigma Aldrich, Malaysia. Pyridine (purity: $\geq 99\%$) was purchased from Merck, Malaysia while ethanol used was from HmbG Chemicals (purity: $>95\%$). All chemicals were of analytical grade and used without further purification.

2.2 Synthesis of benzoyl κ -carrageenan

Bz- κ car was prepared with new synthesis route. Series of κ car: BC mass ratios were prepared (1:0, 1:1, 1:3, 1:5, 1:7 and 1:9). Some modification parts are similar to a previously reported acylated chitosan method [16]. κ car powder was soaked and stirred in pyridine for 24 hours at 50°C for good dispersion. Then, liquid BC was soaked and stirred in pyridine until dissolved at 60°C . The mixture of pyridine and BC was added dropwise into the κ car mixture in 2 hours while being stirred continuously at 60°C . Then, the mixed solution was heated to 60°C under reflux and a heterogeneous product aggregation was observed in the final solution. Pale yellow solution was filtered by a vacuum pump and washed thoroughly with ethanol to

remove excess pyridine. Light yellow powder sample was obtained and dried overnight in the oven. To finish, the powder sample was stored in air tight container until further use.

The synthetic procedure of benzoyl carrageenan synthesis is shown in Figure 1. Herein, the hydrogen atom in the hydrophilic hydroxyl group (-OH) is suggested to be substituted with benzoyl molecule (C₆H₅CO-), through electrophilic substitution (acylation) reaction.

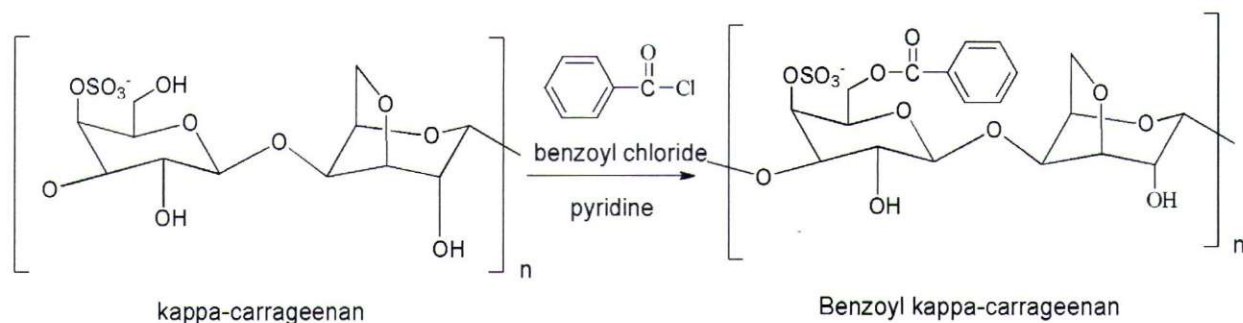
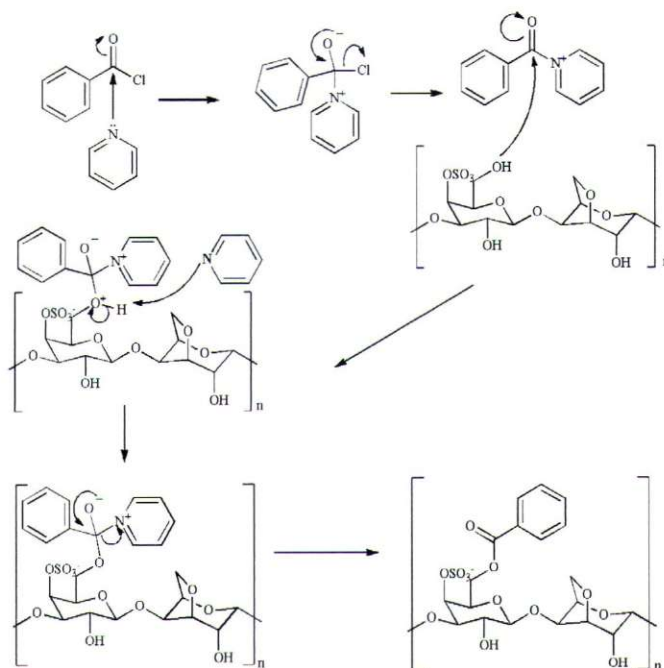


Figure 1: Synthetic procedure of Bz-kcar.

In this synthesis, benzoyl chloride acts as an electrophile and acylating agent that delivers benzoyl molecule into kcar polymeric chain. Pyridine served as nucleophile for carbonyl groups and catalyst in this acylation reaction. The nitrogen atom in pyridine is nucleophilic as the lone pair of electrons on nitrogen cannot be delocalized around the ring. The reaction initiated with pyridine performed nucleophilic attack on the carbonyl group to form benzoyl pyridinium salt. The carbonyl groups are then activated towards nucleophilic attack by the hydroxyl group in kcar. Next step is the deprotonation by pyridine and removal of pyridine as good leaving group. Thus, Bz-kcar is produced as the final product. The complete proposed mechanism is shown in Scheme 1.



Scheme 1. Proposed reaction mechanism for the benzoylation of kcar.

2.3 Preparation of kcar and Bz-kcar gels

Both kcar and Bz-kcar soft gel samples were prepared by dissolving each sample powder in ethylene glycol at the concentration of 3.3% w/v at ambient temperature. The thick gels were stirred overnight in order to obtain complete dissolution. The dissolved gel then kept in air tight container to prevent any moisture contact.

3. Characterization

3.1 Fourier Transform Infra-Red Analysis (FTIR)

The analysis was performed by using Perkin- Elmer Spectrum 2000, USA in the range of 4000-650 cm^{-1} with scanning resolution 4 cm^{-1} . The analyses were carried out to investigate any peak shifts and changes on the spectra due to the chemical interaction between polymer kcar and BC salt.

3.2. Elemental analyzer

The percentage of carbon (C), and sulphur (S) for kcar and Bz-kcar powders were analyzed by using Vario el III, ELEMENTAR, Hanau, Germany. The degree of substitution was calculated based on equation (1) [13]:

$$\text{Degree of substitution} = \frac{\text{ratio carbon: sulphur}_{\text{Bz-kcar}} - \text{ratio carbon: sulphur}_{\text{kcar}}}{\text{number of new added carbon}} \quad (1)$$

3.3 $^1\text{H-NMR}$ spectroscopy

$^1\text{H-NMR}$ spectra were recorded on a Bruker Advance III HD 400 MHz spectrophotometer. Intact samples of kcar powder was dissolved in D_2O and Bz-kcar was dissolved in deuterated dimethylsulfoxide (DMSO-d_6). Samples were transferred into a static magnetic field to excite the nuclei and measure the emitted frequencies.

3.4 X-Ray Diffraction (XRD)

A Bruker D8 Advance X-ray diffractometer was used to analyze the degree of crystallinity of kcar and Bz-kcar powders. The data were collected from a range of diffraction angle 2θ from 3° to 60° at the rate $0.05^\circ \text{ s}^{-1}$. The crystallinity index (X_{CI}) has been calculated using peak separation software EVA. Amorphous subtraction method has been used in calculating the X_{CI} of the biopolymer electrolytes [17]. The amorphous contribution of kcar has been subtracted from the diffraction spectra. Then, X_{CI} was calculated from the ratio of the remaining diffractogram area due to crystalline kcar and the total area of the original diffractogram. The determination of X_{CI} is shown in equation (2):

$$X_{CI} = \frac{A_c}{A_t} \quad (2)$$

where X_{CI} referring to the crystallinity index of the biopolymer, A_c represents the crystalline area and A_t represents the total area of the diffractogram.

3.5 Thermogravimetric analysis (TGA)

A Simultaneous Thermal Analyser (STA) brand NETZSCH model STA 449 F3 Jupiter was used to investigate the thermal behavior of the polymers. Both kcar and Bz-kcar powder samples with a mass of (3- 5 mg) were tested under nitrogen gas atmosphere at a heating rate of $10^\circ\text{C}/\text{min}$ at a temperature range from 30°C - 600°C .

3.6 Solubility test

The solubilities of kcar and Bz-kcar powders were evaluated in multiple solvents: pure water, acetonitrile, tetrahydrofuran, pyridine, dimethyl sulfoxide and acetic acid (99.9% purity). All samples were prepared at the concentration of 1.0% w/v and stirred overnight at 25 °C. The solution was filtered and dried to determine the amount of undissolved sample left. Solubility percentage was calculated based on equation (2).

$$\text{Solubility (\%)} = \frac{\text{mass of sample after dissolution (g)}}{\text{mass of sample before dissolution (g)}} \times 100\% \quad (2)$$

3.7 Water contact angle

The water contact angle of the kcar and Bz-kcar gel samples were measured using The Ossila Contact Angle Goniometer (model L2004A1) with angle range of 5° to 180°. A thin layer of gels was spread on a slide glass (75 mm x 25 mm) and fixed on the horizontal movable stage (50 mm x 50 mm). The WCA was measured soon after dropping an ultra-pure water drop (10 µL) using Eppendorf micropipette.

3.8 Impedance spectroscopy

Impedance spectra was measured using a high-frequency response analyser (HFRA: Solartron 1296) with frequency ranging from 100 Hz to 1MHz with 100 mV amplitude. A dip-cell probe for gel sample was used to measure the conductivity of kcar and Bz-kcar gel samples. The cell constant was determined with a solution of 0.01 M KCl at ambient temperature (298 K).

4. Results and Discussion

The FTIR spectra of kcar and synthesized kcar powders with different ratios of BC (kcar:BC - 1:0, 1:1, 1:3, 1:5, 1:7 and 1:9) are shown in Figure 2. The characteristic peaks at 922 cm⁻¹ is attributed to C-O-C vibration of the 3,6-anhydro-D-galactose residue, while the intense peak at 1037 cm⁻¹ represents the C-O stretching mode in kcar. Peaks at 1231 cm⁻¹ and 844 cm⁻¹ were assigned to O=S=O symmetric vibration and to -O-SO₃ stretching vibration at the C-4 position of galactose in the kcar polymer chain respectively [18].

In order to confirm the benzoyl molecule (C₆H₅CO-) substitution into kcar chains, changes on the FTIR signals were observed. Based on Fig. 2(a), a broad stretching vibration of hydroxyl group (OH band) in kcar powder (ratio 1:0) is detected at around 3200 – 3600 cm⁻¹. As the ratio of benzoyl chloride increases (ratio 1:1-1:9), the intensity of the broad OH band is noticed to be reduced, thus indicating the decrement of hydroxyl bond in the kcar structure. This observation might be related to the electrophilic substitution of hydrogen atom in the -OH group with C₆H₅CO- molecule leading to disruption of hydrogen bonds in the polymer matrix thus signifying the reduction of hydrophilic nature in the synthesized kcar.

The further confirmation of benzoyl substitution is shown in Figure 2(b) by the appearance of several new bands in the synthesized ratio 1:3, 1:5, 1:7 and 1:9. New carbonyl (C=O) stretch peak appeared at 1716 cm⁻¹ [13]. The intensity of the C=O signal is enhanced with higher ratio of BC salt indicating successful substitution of C₆H₅CO- occurred. A pair of new peak is also detected at 1451 and 1605 cm⁻¹ bands belongs to the aromatic C=C stretch [19], thus confirming the successful substitution of C₆H₅CO- into the kcar matrix. Noticeably, a new C-Cl peak is formed at 710 cm⁻¹ in higher ratios; (1:5, 1:7 and 1:9), which might be due to the excess of BC salt in the synthesized kcar.

Significant shifts in the wavenumbers in pure kcar (ratio 1:0) and kcar with increasing ratios of BC salt (ratio 1:1 – 1:9) were observed. Stretching modes in C-O-C and C-O in the synthesized kcar were shifted slightly to higher and lower wavenumbers respectively. The O=S=O symmetric vibration band also showed significant changes as the band shifted to higher wavenumbers. The shifts of the characteristic

bands might be caused by the coordination interaction of oxygen atoms as electron rich species in the polymer matrix with the hydrogen ion (H^+) that is detached from the hydroxyl bond as a result of the acylation reaction. Hence, these changes suggest the successful substitution of benzoyl molecule in the kcar matrix. The summarized shifts and assignments of the individual characteristic bands are shown in Table 1. Based on all these IR peak changes, we conclude that Bz-kcar has been produced.

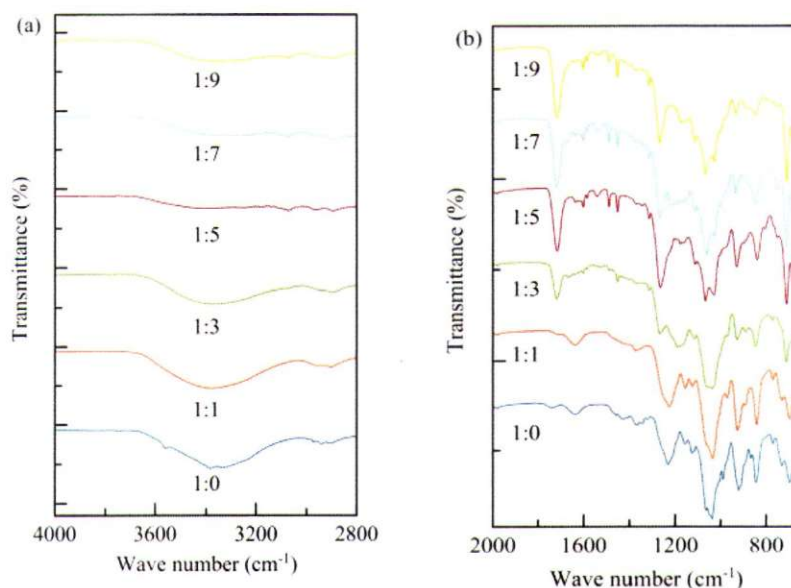


Figure 2: FTIR spectra of different ratios kcar: BC (1:0, 1:1, 1:3, 1:5, 1:7 and 1:9) at (a) 4000- 2800 cm^{-1} and (b) 2000- 650 cm^{-1} .

Table 1: The assigned bands and wavelength of the synthesized kcar powders.

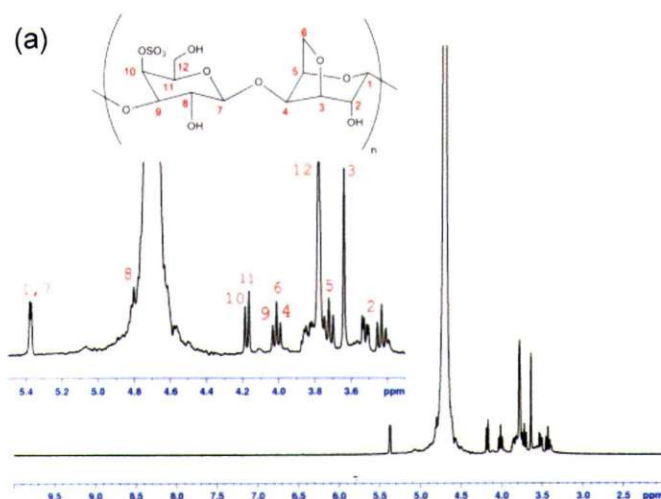
Assignments of bands	kcar: BC ratio					
	Wavelength (cm^{-1})					
	1:0	1:1	1:3	1:5	1:7	1:9
O-H	3384	3381	3374	3368	3327	3378
C-O-C	921	926	927	929	933	933
C-O	1037	1036	1036	1028	1027	1027
O=S=O	1231	1224	1267	1267	1267	1268
C=O	None	None	1718	1716	1716	1716
C=C	None	None	1452,1602	1451,1602	1451,1602	1451,1602
C-Cl	None	None	711	710	710	708

The elemental analysis of C and S for series of kcar: BC ratios are tabulated in Table 2. The analysis displayed higher percentage of C as the ratios of BC salt increase. This suggests that the synthesized kcar has reacted with BC salt and benzoylation has taken place in kcar matrix. The upmost percentage of C is observed in the ratio 1:5 of kcar: BC, an increase of 35% compared to the pristine kcar (ratio 1:0). The degree of substitution (DS) were calculated based on equation (1) by comparing the C and S ratio obtained from element analysis in each ratio. Notably, ratio 1:5 showed the highest degree of substitution (DS) at 0.27, suggesting ratio 1:5 of kcar: BC contains the highest benzoyl substitution in kcar matrix and implies as the most ideal ratio for the synthesis. The DS started to decrease as higher amount of BC salt was included (ratio 1:7 and 1:9) which could be caused by the saturation or agglomeration of BC salt in the polymer matrix thus hinder the substitution to occur.

Table 2: Elemental analysis and DS of synthesized kcar.

kcar: BC sample	C (%)	S (%)	C/S	DS
1:0	28.00	4.70	5.96	-
1:1	28.30	4.60	6.15	0.03
1:3	32.50	5.00	6.50	0.08
1:5	37.90	4.75	7.98	0.27
1:7	37.20	4.90	7.59	0.23
1:9	37.80	5.20	7.27	0.19

Further evidence of benzoyl substitution into kcar matrix is supported by $^1\text{H-NMR}$ spectroscopy. $^1\text{H-NMR}$ spectroscopy has the advantage of high selectivity and suitable for quantitative approximation for different types of carrageenan [20]. The $^1\text{H-NMR}$ spectra of kcar and Bz-kcar (ratio 1:5) samples are shown in Fig. 3 (a and b) respectively (chemical shift ranging between $\delta = 2.0$ and 10.0 ppm). Proton signals of kcar backbone (Fig. 3a) appear at range 3.45-5.38 ppm and the chemical shifts could be assigned as follows: $^1\text{H-NMR}$ (D_2O): $\delta = 5.37$ (H1), $\delta = 3.52$ (H2), $\delta = 3.63$ – 3.69 (H3), $\delta = 3.98$ (H4), $\delta = 3.50$ – 3.53 (H5), $\delta = 4.01$ (H6), $\delta = 5.36$ (H7), $\delta = 4.81$ (H8) $\delta = 4.03$ (H9), $\delta = 4.18$ (H10) $\delta = 4.16$ (H11) and $\delta = 3.77$ (H12), comparable with previous studies [13, 14]. Chemical shifts spectrum of Bz-kcar (Fig. 3b) showed similar characteristic to kcar proton signals with appearance of new multiple resonances peaks ($\delta = 6.6$ – 9.50 ppm) belongs to the characteristic signals of protons in aromatic benzoate group ($\text{C}_6\text{H}_5\text{CO}$ -). Similar proton signals of benzoylated derivatives were published [17, 21]. These findings proved the electrophilic substitution of benzoyl group into kcar matrix and supported the FTIR analysis. Thus, this has also confirmed that the synthesis was successfully accomplished.



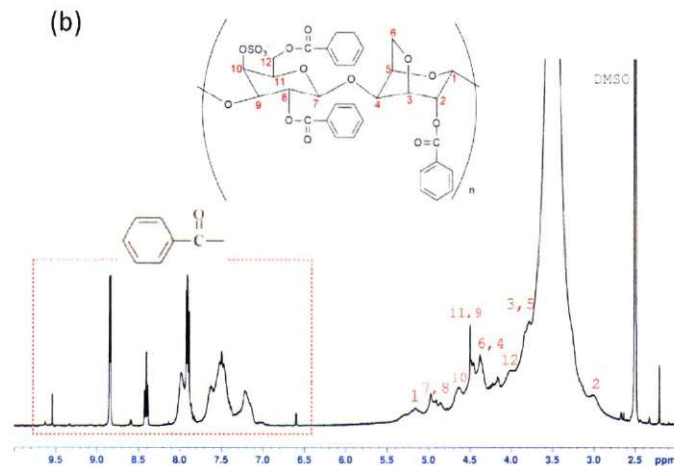


Figure 3: ¹H-NMR spectra of (a) kcar and (b) Bz-kcar.

Fig. 4 shows the X-ray diffraction pattern of pure kcar powder and Bz-kcar powder (ratio 1:5). Observably, the nature of pure kcar film is semicrystalline, with a small hump at $2\theta = 2.0 - 10.0^\circ$ and a broad hump at around $2\theta = 12.0 - 41.0^\circ$. Sharp peaks were shown at $2\theta = 29.0^\circ$ and 41.0° similar to the conventional characteristic diffraction peaks of kcar reported [22, 23].

Modification of kcar has exhibited significant changes in the structural phase of the biopolymer as displayed in the diffractogram of Bz-kcar (Fig. 5(b)). Noticeably, there were multiple formation of new peaks ranging at $2\theta = 9.0 - 37.0^\circ$ with accentuated peaks at $2\theta = 12^\circ, 14^\circ, 19^\circ, 25^\circ, 32^\circ$ and 37° . The appearance of these new peaks is probably due to the engagement of crystalline benzoyl molecule in the biopolymer backbone, that leads to the formation of polymer–benzoyl complexes as the optimum amount of benzoyl chloride was included. Residue of unreacted benzoyl chloride might have also been the cause. Comparable trend was observed in the synthesization of acylated chitosan derivatives [24].

Observably, upon modification, the small hump at $2\theta = 6.0 - 12.0^\circ$ has not been significantly changed. However, reduced intensity with disordered structure of the synthesized Bz-kcar (Fig. 5(b)) as compared to the pristine kcar (Fig. 5(a)) is observed at $2\theta = 10.0 - 40.0^\circ$. This observation might be related to the electrophilic substitution of the hydroxyl (OH) group with aromatic benzoyl (C_6H_5-CO-) molecule in the kcar matrix (Scheme 1). Consequently, there were disruption of inter and intramolecular hydrogen bonding in the biopolymer matrix thus resulted in the disordered arrangement in the synthesized benzoyl kcar chain. The disordered structural arrangement has then affected the crystallinity of the biopolymer as the crystallinity index (X_{CI}) of benzoyl kcar was found to lessened at 24.3% as opposed to the pure kcar, 26.7%. Thus, this has also shown that the modification of kcar has arranged the polymer chain structure whereby the new arrangement has enhanced the formation of amorphous phase. Table 3 shows the percentages of X_{CI} and amorphous in kcar and Bz-kcar.

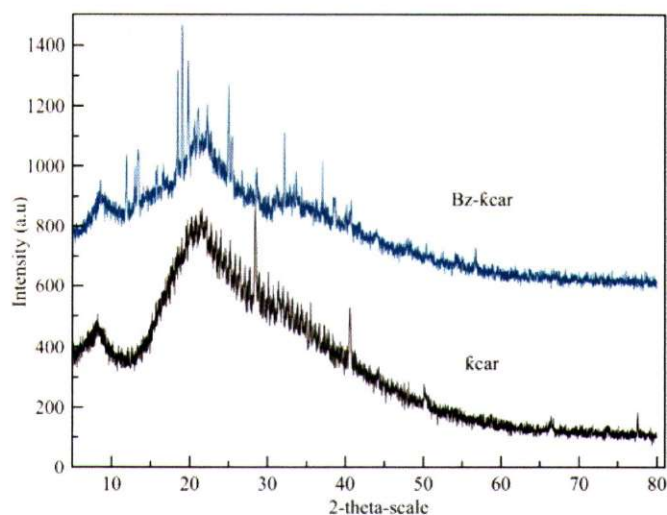


Figure 4: XRD pattern of kcar and Bz-kcar powders.

Table 3: Crystallinity index and amorphous percentages of kcar and Bz-kcar.

Sample	Crystallinity index, X_{Cl} (%)	Amorphous (%)
kcar	26.7	73.3
Bz-kcar	24.3	75.7

The TGA and DTG curves of kcar and Bz-kcar are shown in Fig. 5. Based on the figure, three distinct stages of weight losses were observed in kcar, while Bz-kcar showed two stages of weight losses. The first weight loss stage in kcar is about 5.2% at temperature range of 40 and 140 °C. Bz-kcar showed lower weight loss approximately 4.8% at similar temperature range. These initial weight losses are due to the presence of moisture in the samples and related to the characteristic of polysaccharides that have strong affinity for water [9]. Reduced moisture weight loss in Bz-kcar is related to its less hydrophilicity characteristic due to the acylation of benzoyl molecule and disruption hydrogen bonding in the polymer chain thus reduce polar interactions with water molecules.

Second degradation peak of kcar was found at temperature peak 222.9 °C with small weight loss about 6.1%, followed by the third degradation stage started at 231.0 °C and reached a maximum at 251.8 °C. The synthesized polymer, Bz-kcar exhibited lower degradation temperature which maximum degradation peak appeared at 205.9 °C with 58% weight loss. This degradation step was identified as devolatilization step where the main pyrolytic process occurred and various volatile components may release gradually. According to previous study, this degradation step was attributed to the loss of $-SO_3-$ group from the pendant chains attached to the polymeric backbone and also may be due to the polysaccharide backbone fragmentation [25, 26]. Noticeably, the second degradation temperature of the acylated kcar were lower compared to the original biopolymer. This might be due to the effect of disruption of hydrogen bonding in the molecule chains, thus leading to disordered structure and the reduced crystallinity of Bz-kcar as discussed in the structural analysis part. Therefore, less energy was needed for

Bz-kcar to degrade. Nevertheless, the degradation temperature of the Bz-kcar is still favorable and suitable to be applied for industrial application.

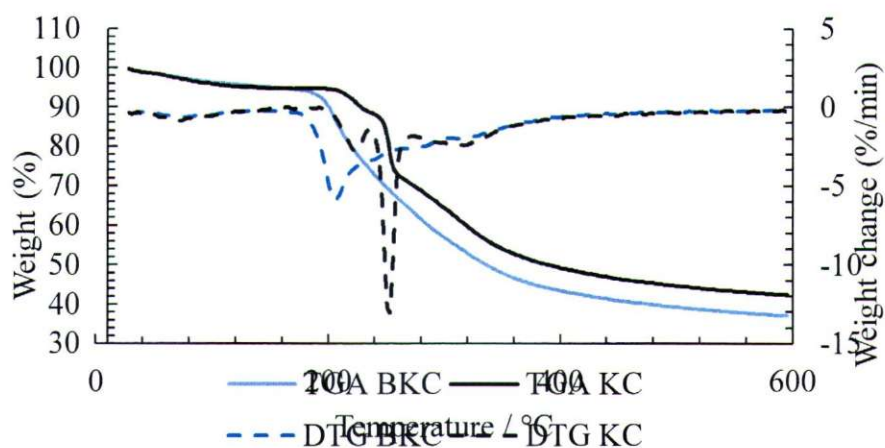


Figure 5: TGA and DTG curves of kcar and Bz-kcar.

To examine the effects of the benzoyl substitution on kcar's hydrophilicity, solubility test on kcar and Bz-kcar powders in several solvents with vary range polarity indices were performed. Solubility is regarded as the ability of solute to form solution with solvent. Table 4 displays solubility percentages of kcar and Bz-kcar in seven different solvents. Generally, the higher the polarity index, the more polar the solvent is, as a result of the strong hydrogen bonds in the molecule [27].

Noticeably, the original polymer, kcar, showed complete dissolution in both highly polar solvents; water and dimethyl sulfoxide (DMSO). On the other hand, Bz-kcar showed reduced solubility percentage in both water and DMSO. A decrease of ~38% solubility is observed in water, while ~85% Bz-kcar dissolution is observed in DMSO, signifying the reduced polarity of Bz-kcar compared to the original kcar. These findings might be due to the interrupted hydrogen bonds in Bz-kcar resulted in reduced polar groups in the polymer chain, thus limit the interactions with the polar solvents. Complete dissolution of Bz-kcar is observed in ethylene glycol (EG), suggesting EG as the most ideal solvent for Bz-kcar. The high solubility of Bz-kcar in EG is most likely related to the semi-polar characteristic of Bz-kcar, as the strong inter and intramolecular hydrogen bonds in the polymer chains are not entirely destroyed. This explains the relatively low degree of substitution (DS) in Bz-kcar as discussed in the elemental analysis part.

Low percentages in solubility are detected in the less polar solvents for both kcar and Bz-kcar. Better dissolution in acetic acid is observed in kcar, as opposed to Bz-kcar. Whereas, the synthesized Bz-kcar portrayed improved solubility percentage trend in solvents with low polarity values (acetonitrile, pyridine and THF), indicating its less polar behavior compared to kcar. These findings have proven that the acylation of benzoyl molecule into the polymer chains has altered its physical characteristic. Reduced solubility in highly polar solvents and better dissolutions in less polar solvents were achieved as a result of the reduced polarity and hydrophilicity in Bz-kcar. Hence, accomplish our aim in this study.

Table 4: Solubility percentages of kcar and Bz-kcar in different solvents.

Solvent	Polarity index [28, 29]	Solubility (%)	
		kcar	Bz-kcar
H ₂ O	10.2	100	62
DMSO	7.2	100	85
Ethylene glycol	6.9	75	100
Acetic acid	6.0	24	18
Acetonitrile	5.8	5	20
Pyridine	5.3	23	27
THF	4.0	6	13

The WCA of kcar and Bz-kcar gels are shown in Figure 5(a) and 5(b) respectively while the WCA data analysis are shown in Table 5. The polynomial fit of the unmodified gel, kcar, showed a very low average angle of 15.31°, signifying its highly hydrophilic properties as WCA smaller than 90° generally signifies a surface having the affinity toward the liquid [30]. However, the average WCA of synthesized Bz-kcar gel increased to 26.52° indicating reduced hydrophilicity of Bz-kcar gel. The reduced hydrophilicity of Bz-kcar was mainly due to its reduced interaction with water molecules as a result of the interrupted inter and intramolecular hydrogen bonds in its polymer matrix. The substitution of hydrophobic benzoyl group in Bz-kcar matrix might had also hindered the polymer interaction with water molecules. The low WCA value in both kcar and Bz-kcar is most likely related to the gelled form of the polymers, as ethylene glycol was applied as the solvent and has strong affinity towards water molecules. The left and right root mean square error (RMSE) values for both polymer gels are below than 1.0 indicating the simulated angle values are in good fits.

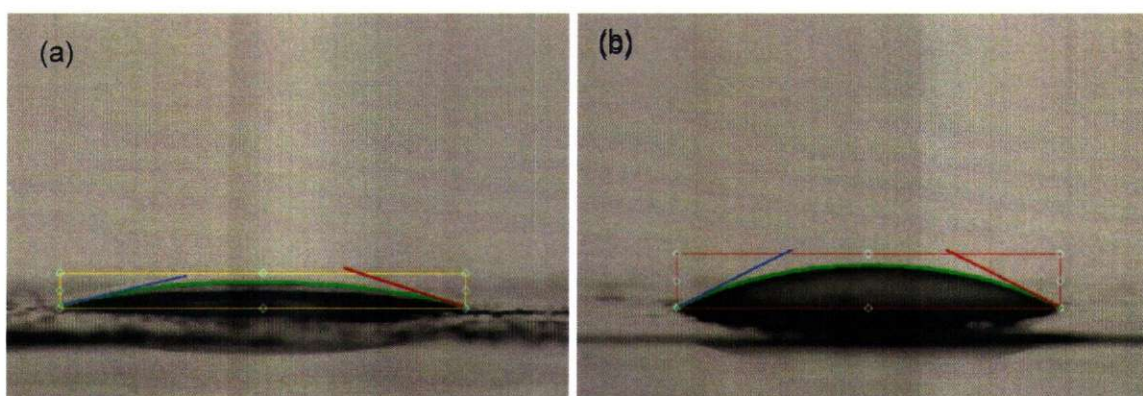


Figure 6: Water contact angles of (a) kcar and (b) Bz-kcar.

Table 5: WCA analysis of kcar and Bz-kcar.

Gel	Left Angle (°)	Right Angle (°)	Average Angle (°)	Left RMSE	Right RMSE
kcar	13.06	17.57	15.31	0.47	0.58
Bz-kcar	26.55	26.48	26.52	0.38	0.38

Electrochemical impedance spectroscopy is an analysis to determine the ionic conductivity (σ). The Nyquist plots of kcar and Bz-kcar gels are shown in Figure 7. The bulk resistance (R_b) was determined from the interception of the tilted spike at the real impedance axis (Z'). Bz-kcar gel displayed smaller R_b value as compared to kcar gel indicating higher value of σ . Figure 8 illustrated the conductivity of both pristine and synthesized polymers at ambient temperature (298 K). It is observed that the σ of synthesized Bz-kcar is higher than its pristine kcar. The σ of kcar achieved was $8.20 \times 10^{-5} \text{ Scm}^{-1}$, while the σ of Bz-kcar showed an increment close to 1 magnitude to $3.10 \times 10^{-4} \text{ Scm}^{-1}$. This has proven that the acylation of benzoyl molecule into kcar matrix has improved its σ . This might be related to the disruption of strong hydrogen bonding and reduced crystallinity of Bz-kcar as shown in the FTIR and structural analyses. As the crystallinity decreased, the increase in the amorphous phase has softened the polymer backbone and enhanced the flexibility and segmental motion of the polymer chains [31]. The gel form of Bz-kcar had also contributed to the flexibility of the polymer chain. As a result, the enhancement in the ionic conductivity is perceived. The high σ of Bz-kcar achieved, without inclusion of any charge carrier or cation salt indicates the highly potential of Bz-kcar as a gel polymer host in electrolyte system.

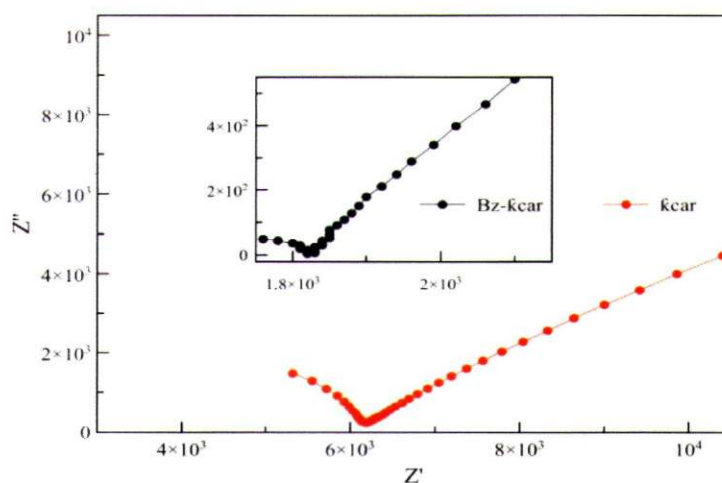


Figure 7: Nyquist plots of kcar and Bz-kcar gels

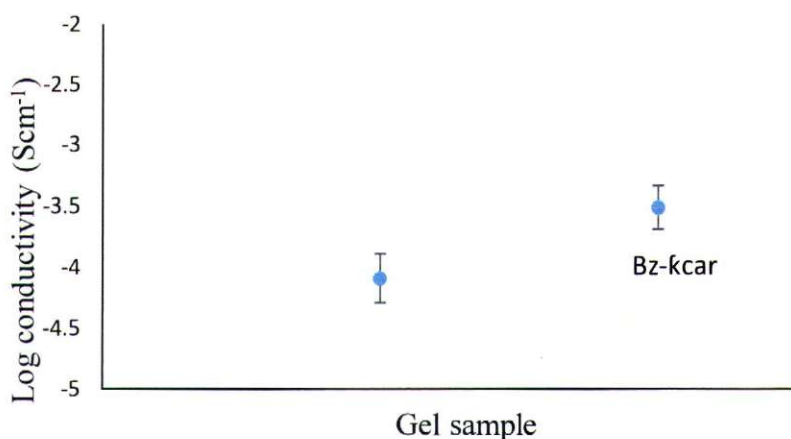


Figure 8: Ionic conductivity, σ of kcar and Bz-kcar gels

5. Conclusions

Benzoyl kappa carrageenan (Bz-kcar), a new kcar derivative with less hydrophilic and improved conductivity has been successfully produced via electrophilic substitution in acylation reaction. Benzoyl chloride was employed as the acylating agent. Pyridine was used as the catalyst and nucleophile source in the reaction. The substitution of aromatic benzoyl molecule into the polymer chain has led to less hydrogen bonding and polar interactions with water molecules, thus reduce the hydrophilicity of Bz-kcar. The chain flexibility of Bz-kcar gel is improved thus increase the ionic conductivity. Bz-kcar has high potential to be applied as a green electrolyte in electrochemical devices. Better performance of Bz-kcar with incorporation of charge carrier such as lithium or sodium salts is anticipated in our next study.

Author Contributions: Conceptualization and project administration, I.J.S; formal analysis, N.S, S.A.M.N, investigation, N.S; methodology, H.H, N.K, S.T, resources, N.K, S.T; supervision, I.J.S, H.H, N.K, S.A.M.N, writing – original draft, N.S, writing – review and editing, I.J.S, H.H, N.K, S.A.M.N, S.T. All authors have read and agreed to the published version of the manuscript.

Funding: This research was funded by the Ministry of Higher Education Malaysia (M.O.H.E.) and National Defence University of Malaysia (NDUM) (Grant No: RACER/1/2019/STG01/UPNM//2 and UPNM/2021/GPPP/SG/2).

Acknowledgement: The authors would like to thank Research Centre for Chemical Defence (CHEMDEF), National Defence University of Malaysia, for the analytical services provided.

Conflicts of Interest: The authors declare no conflict of interest.

References

1. Campo, V.L., et al., *Carrageenans: Biological properties, chemical modifications and structural analysis—A review*. 2009. **77**(2): p. 167-180.
2. Distantina, S., M.J.I.J.o.C. Fahrurrozi, and M. Engineering, *Carrageenan properties extracted from *Eucheuma cottonii*, Indonesia*. 2011. **5**(6): p. 501-505.
3. Hotchkiss, S., et al., *The use of carrageenan in food*. 2016: p. 229-243.
4. Infante, V.H.P., P.M.M.J.I.J.o.P. Campos, and N. Ingredients, *Application of factorial design in the development of cosmetic formulations with carrageenan and argan oil*. 2021. **8**(1): p. 4-4.
5. Pacheco-Quito, E.-M., R. Ruiz-Caro, and M.-D.J.M.D. Veiga, *Carrageenan: drug delivery systems and other biomedical applications*. 2020. **18**(11): p. 583.
6. Kazda, T., et al., *Carrageenan as an Ecological Alternative of Polyvinylidene Difluoride Binder for Li-S Batteries*. 2021. **14**(19): p. 5578.
7. Ramírez Sánchez, K., et al., *Polysaccharide κ -carrageenan as doping agent in conductive coatings for electrochemical controlled release of dexamethasone at therapeutic doses*. 2020. **25**(9): p. 2139.
8. Lu, J., et al., *Recent Progress in Quasi-Solid and Solid Polymer Electrolytes for Multivalent Metal Ion Batteries*. 2021.
9. Tecante, A. and M.J.R. Nunez Santiago, *Solution properties of κ -carrageenan and its interaction with other polysaccharides in aqueous media*. 2012. **1**: p. 241-264.
10. Ellis, A., et al., *The hydrophobic modification of kappa carrageenan microgel particles for the stabilisation of foams*. 2019. **538**: p. 165-173.
11. Tye, Y.Y., et al. *Preparation and characterization of modified and unmodified carrageenan based films*. in *IOP Conference Series: Materials Science and Engineering*. 2018. IOP Publishing.
12. Mahmood, W.A.K., M.M.R. Khan, and T.C.J.J.o.P.S. Yee, *Effects of reaction temperature on the synthesis and thermal properties of carrageenan ester*. 2014. **25**(1): p. 123.
13. Abu Bakar, M.H., et al., *Effect of active site modification towards performance enhancement in biopolymer κ -Carrageenan derivatives*. 2020. **12**(9): p. 2040.
14. Liew, J.W.Y., et al., *Synthesis and characterization of modified κ -carrageenan for enhanced proton conductivity as polymer electrolyte membrane*. 2017. **12**(9): p. e0185313.
15. Mobarak, N., et al., *Chemical interaction and conductivity of carboxymethyl κ -carrageenan based green polymer electrolyte*. 2012. **224**: p. 51-57.

16. Zong, Z., et al., *Characterization of chemical and solid state structures of acylated chitosans*. 2000. **41**(3): p. 899-906.
17. Chen, W., et al., *Homogeneous benzylation of cellulose in 1-allyl-3-methylimidazolium chloride: Hammett correlation, mechanism and regioselectivity*. 2015. **5**(72): p. 58536-58542.
18. Pereira, L., et al., *Identification of selected seaweed polysaccharides (phycocolloids) by vibrational spectroscopy (FTIR-ATR and FT-Raman)*. 2009. **23**(7): p. 1903-1909.
19. Bardakçı, B. and S.J.Z.f.N.A. Bahçeli, *An IR study of benzoyl chloride adsorbed on KA, NaA, and CaA zeolites*. 2005. **60**(8-9): p. 637-640.
20. Lankhorst, P.P. and A.-N.J.S.I.P.A.C. Chang, Switzerland, *The application of NMR in compositional and quantitative analysis of oils and lipids*. 2018: p. 1743-1764.
21. Namyslo, J.C., M.H. Drafz, and D.E.J.P. Kaufmann, *Durable Modification of Wood by Benzylation—Proof of Covalent Bonding by Solution State NMR and DOSY NMR Quick-Test*. 2021. **13**(13): p. 2164.
22. Christopher Selvin, P., et al., *Study of proton-conducting polymer electrolyte based on K-carrageenan and NH₄SCN for electrochemical devices*. 2018. **24**(11): p. 3535-3542.
23. Zainuddin, N., et al., *Characterization on conduction properties of carboxymethyl cellulose/kappa carrageenan blend-based polymer electrolyte system*. 2018. **23**(4): p. 321-330.
24. Ma, G., et al., *Synthesize and characterization of organic-soluble acylated chitosan*. 2009. **75**(3): p. 390-394.
25. Mishra, D.K., J. Tripathy, and K.J.C.P. Behari, *Synthesis of graft copolymer (k-carrageenan-gN, N-dimethylacrylamide) and studies of metal ion uptake, swelling capacity and flocculation properties*. 2008. **71**(4): p. 524-534.
26. Mishra, M.M., et al., *Water soluble graft copolymer (κ-carrageenan-gN-vinyl formamide): Preparation, characterization and application*. 2010. **80**(1): p. 235-241.
27. Marcus, Y. and Y.J.T.J.o.P.C. Migron, *Polarity, hydrogen bonding, and structure of mixtures of water and cyanomethane*. 1991. **95**(1): p. 400-406.
28. Barwick, V.J.J.T.T.i.A.C., *Strategies for solvent selection—a literature review*. 1997. **16**(6): p. 293-309.
29. Gupta, M.N., et al., *Polarity index: the guiding solvent parameter for enzyme stability in aqueous-organic cosolvent mixtures*. 1997. **13**(3): p. 284-288.
30. Hebbar, R., A. Isloor, and A. Ismail, *Contact angle measurements*, in *Membrane characterization*. 2017, Elsevier. p. 219-255.
31. Zhu, M., et al., *Recent advances in gel polymer electrolyte for high-performance lithium batteries*. 2019. **37**: p. 126-142.